Supporting Information:

Relationship between Lewis acid sites and carbohydrate reactivity over Sn-β catalysts

*Yacine Boudjema, Antoine Brunel, Raphaël Del Cerro, Gerhard Pirngruber, Céline Chizallet and Kim Larmier**

IFP Energies nouvelles, Rond-Point de l'Echangeur de Solaize, 69360 Solaize, France

Email : kim.larmier@ifpen.fr

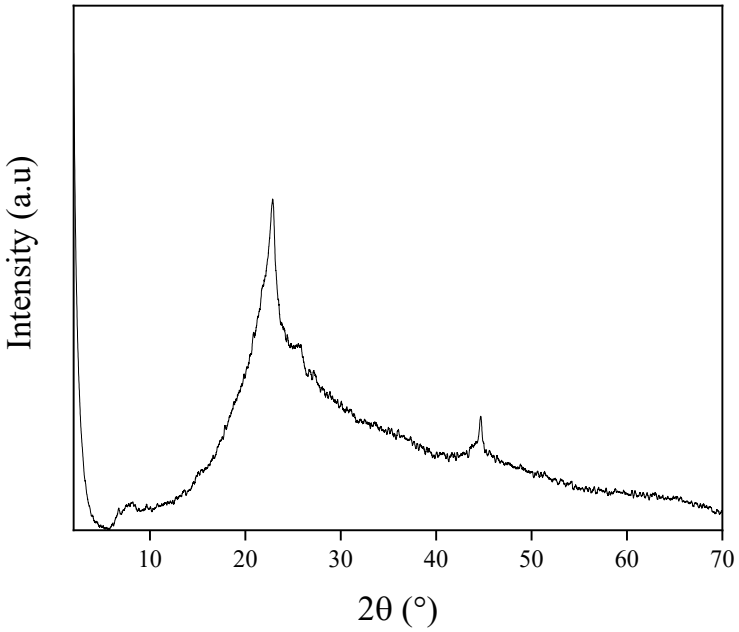

Figure S1. Diffractograms of Sn-β synthetized by hydrothermal method without TEABr.

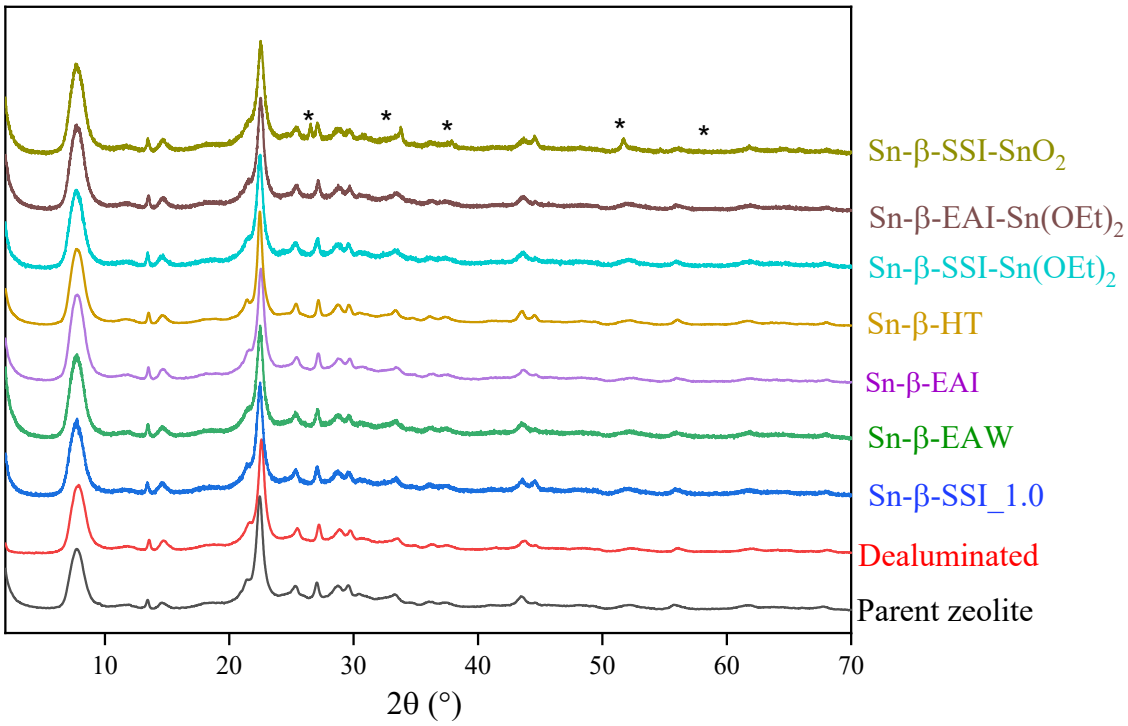

Figure S2. Diffractograms of parent zeolite (black), dealuminated (red) and Sn-β materials.

*: SnO_2 oxide phase, PDF: 04-002-0289.

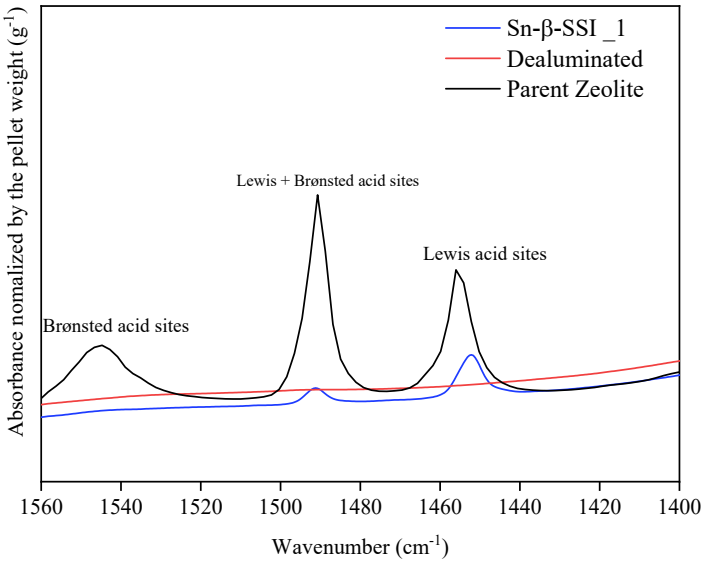

Figure S3. FTIR spectrum of pyridine recorded after desorption at 150 °C with subtraction of the spectrum of the activated sample at 450 °C on Sn-β-SSI_1.0.

Section S1 : Elements of heterogeneous catalysis engineering

Mass transfer limitation

Calculations of diffusion order of magnitude are necessary to assess whether the system is likely to experience significant internal or external diffusion limitations. The case of the catalyst with the highest activity, Sn-β-SSI_1.0 at 150°C will be studied, as it the most susceptible to experience diffusion limitation.

External mass transfer limitations

The order of magnitude for the particle-liquid mass transfer coefficient k_{SL} is typically between 2×10^{-5} and 10×10^{-5} m s^{-1} in the case of a stirred tank reactor with a heterogeneous catalyst in slurry,[1] to be conservative, a value of 1×10^{-5} m s^{-1} will be used.

According to laser granulometry, volume-weighted catalyst grain size has a d_{50} value of 4.1 µm. Therefore, the exchange surface per volume of solution A/V can be estimated assuming spherical particle with a radius (R_p) of 2.05 µm. The specific mass of M-β, ρ_{cat}, was determined to be 1230 kg m^{-3} by mercury porosimetry. Under the conditions employed, the concentration of Sn-β-SSI_1.0 in the liquid phase C_{cat} is 13.2 kg m^{-3} for experiments using glucose as a substrate. The surface-to-volume ratio U of the catalyst for spherical particles can be estimated using relation (1):

$$U = \frac{3}{Rp} \qquad (1)$$

Then, the exchange surface per volume of solution A/V can be expressed by relation (2):

$$\frac{A}{V} = U \times \frac{C_{cat}}{\rho_{cat}} \qquad (2)$$

The characteristic rate of external diffusion $k_{D,ext}$ can be calculated by relation (3):

$$k_{D,ext} = k_{SL} \times \frac{A}{V} \qquad (3)$$

Finally, value of 1.6×10^{-1} s^{-1} is found for glucose conversion using Sn-β-SSI_1.0.

The apparent first order rate constant in glucose consumption in our study using Sn-β-SSI_1.0 as a catalyst at 150°C is 6.5×10^{-4} s^{-1}. This value for glucose conversion is lower than $k_{D,ext}$ by more than one order of magnitude. Hence, external mass transfer limitations may be excluded.

Internal mass transfer limitations

The Weisz-Prater criterion $N_{W\text{-}P}$ can be used to determine if there is severe internal diffusion limitation within the micrometric particles (that constitute agglomerates of small beta cristallites).[2] This criterion is defined as relation (4):

$$N_{W.P} = \frac{r_v \times R_p^2}{C_{glucose} \times D_{Eff}} \qquad (4)$$

where D_{eff} is the diffusion coefficient of glucose in water (7×10^{-10} m^2 s^{-1}),[3] $C_{substrate}$ is the initial concentration of glucose in the liquid phase 113 mol m^{-3} and r_v the apparent reaction rate normalized by the volume of catalyst is 6.9× 10 mol s^{-1} m_{cat}^{-3}. This yields $N_{W\text{-}P}$ of 3.7×10^{-4} for glucose. This value is much lower than the value of 0.3 usually defined to consider the criterion satisfied. Hence, we may consider that no significant internal mass transfer limitations occur under our conditions.

However, it is important to note that this calculation only concerns the diffusion in the intercrystalline space of the particles and does not exclude the possibility of diffusion limitations within the microporous network or the accessibility of the substrate to the active sites.

Section S2 : Equations for the calculation of yields, conversion and carbon balance

$$Carbon\ Balance\ = \frac{\sum_i n(A_i)\ \times\ C_i(t)}{\sum_i n(A_i)\ \times\ C_i(0)}$$

Equation S1. Determination of the carbon balance.

n(A_i): Carbon number in the molecule A_i.

C_i : concentration of species A_i (mol kg^{-1})

$$S_i(t) = \frac{n(A_i) \times C_i(t)}{n(glucose) \times (C_{glucose}(0) - C_{glucose}(t))}$$

Equation S2. Determination of the selectivity.

$$Y_i(t) = \frac{n(A_i) \times C_i(t)}{n(glucose) \times C_{glucose}(0)}$$

Equation S3. Determination of the yield.

$$X_{glucose}(t) = \frac{C_{glucose}(0) - C_{glucose}(t)}{C_{glucose}(0)}$$

Equation S4.Determination of glucose conversion.

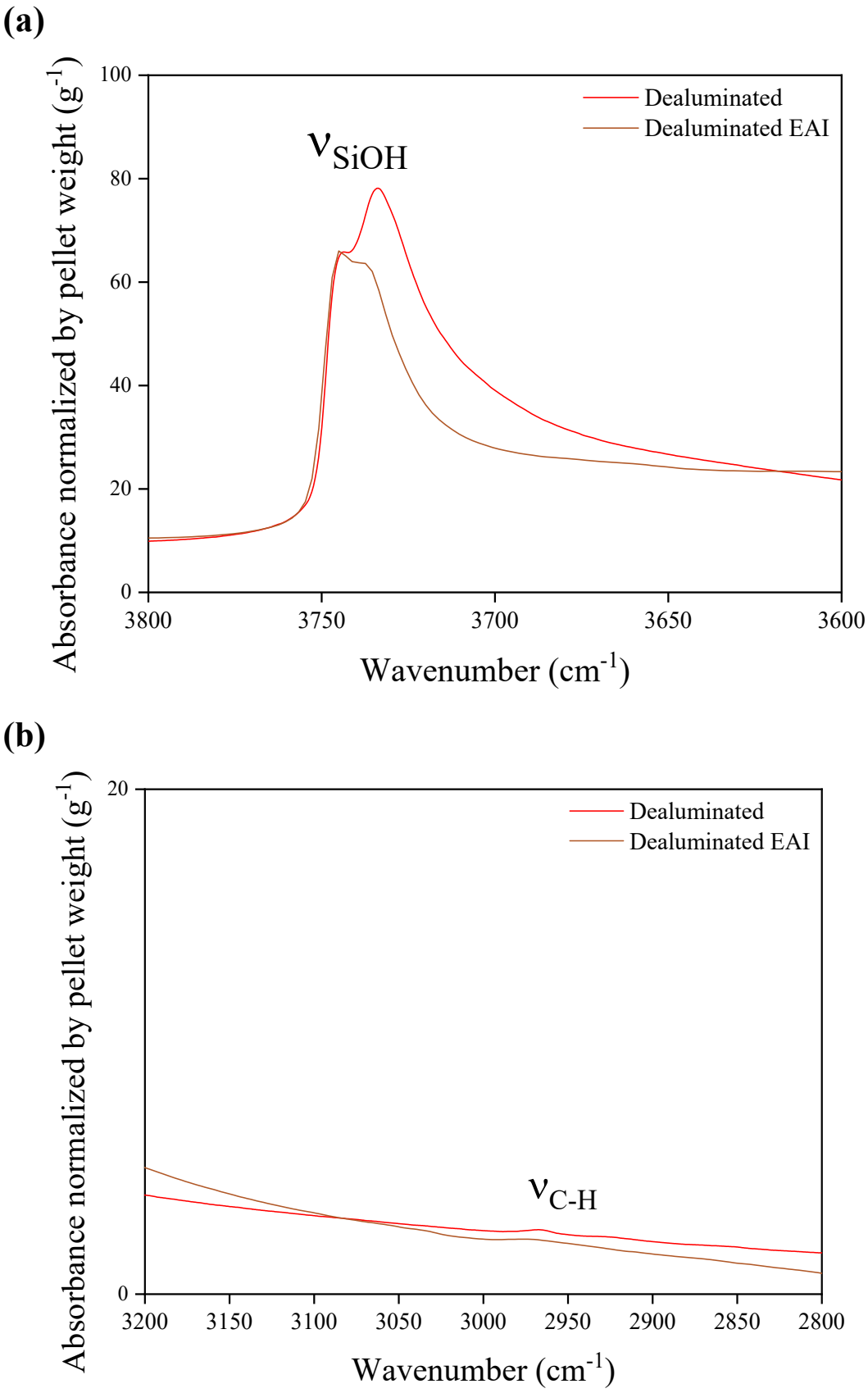

Figure S4. FT-IR spectra after activation of dealuminated (red) and dealuminated after EAI treatment. (a) Zoom on the ν-OH region (b) zoom on the ν-CH region.

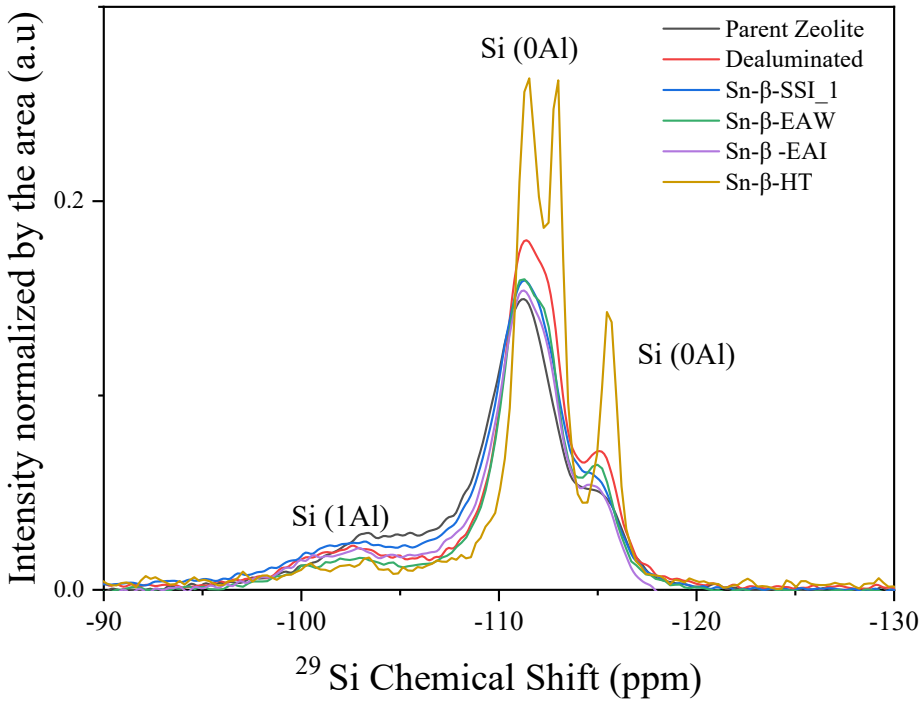

Figure S5. ^{29}Si NMR of aluminosilicate zeolite (black), dealuminated zeolite (red), Sn-β-SSIE_1 (blue), Sn-β-EAW (green) Sn-β-EAI (purple) and Sn-β-HT (yellow). Recycling delay of 20 s

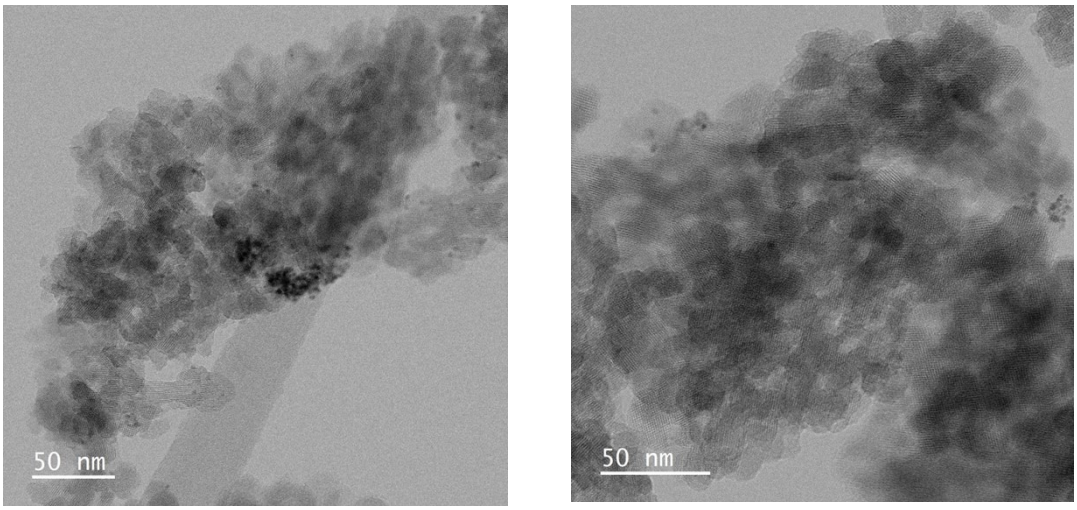

Figure S6. Comparison of the TEM micrographs of Sn-β-EAW before (left) and after (right) washing with water.

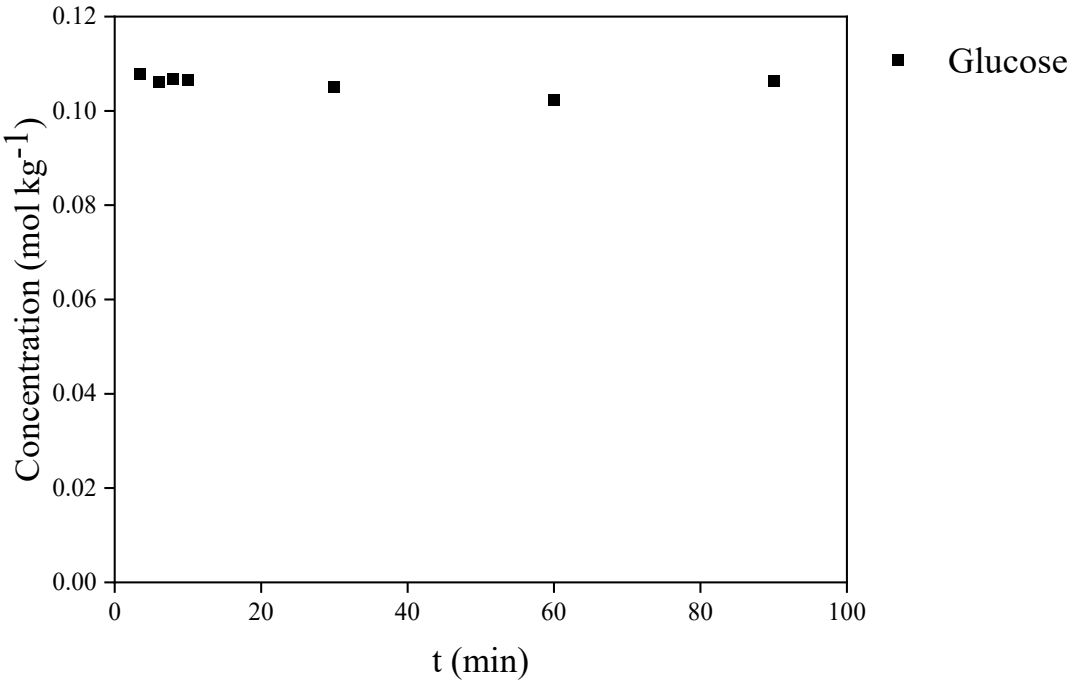

Figure S7. Glucose conversion versus time without catalyst. Reaction conditions: T= 150 °C, P= 40 bar N_2, concentration of glucose 0.1 mol kg^{-1}.

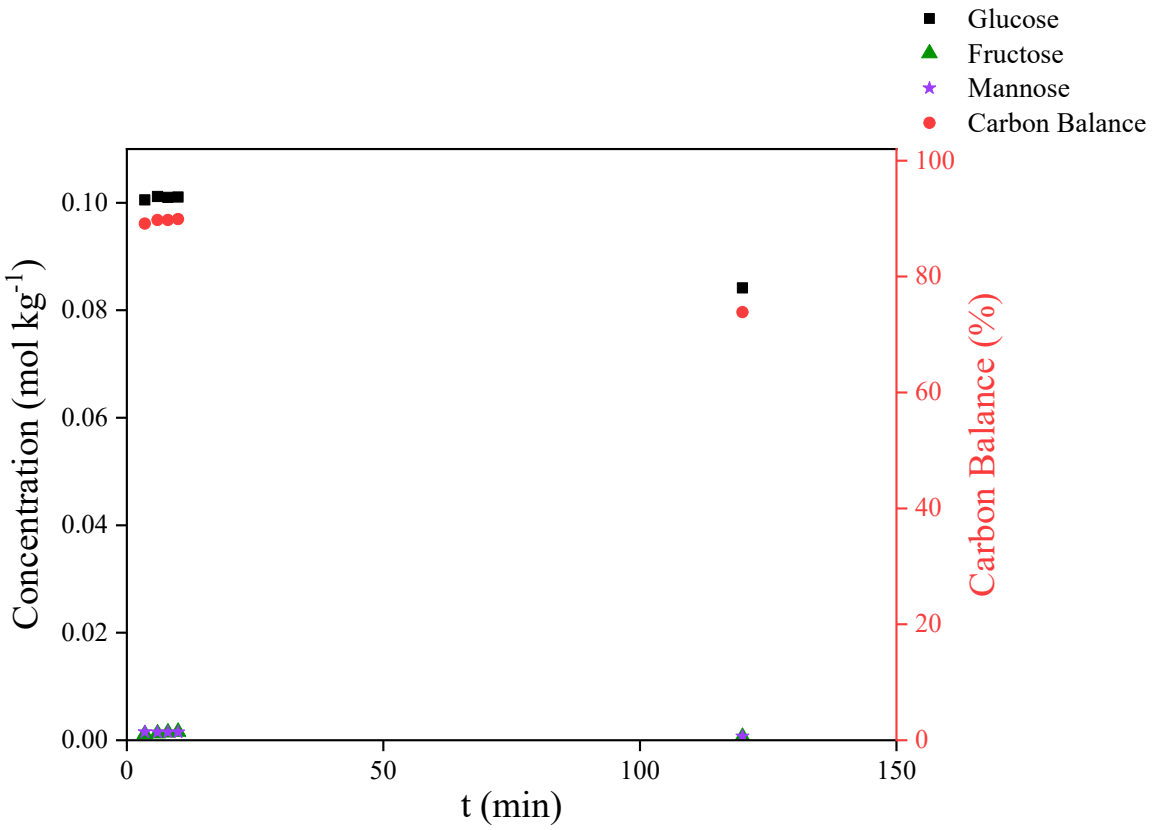

Figure S8. Glucose conversion versus time with calcined parent zeolite. Reaction conditions: T= 150 °C, P= 40 bar N_2, concentration of glucose 0.1 mol kg^{-1} and substrate/metal = 100 mol/mol in water (m_{cat} =0.064 g).

Table S1. Final Carbon Distribution (%) after 120 min of reaction over Sn-β_SSI 1wt%

With calcination between cycle	Glucose	Fructose	Mannose	GLA	DHA	5-HMF	Lactic Acid	Other
Cycle 1	17.7	22.9	8.2	7.4	2.4	7.4	26.7	7.3
Cycle 2	28.4	29.0	13.0	1.0	3.9	5.4	16.4	2.9
Cycle 3	50.2	27.4	7.9	0.7	3.4	2.3	6.7	1.4
Without calcination between cycle	Glucose	Fructose	Mannose	GLA	DHA	5-HMF	Lactic Acid	Other
Cycle 1	17.6	26.1	11.0	3.6	2.6	7.4	28.4	3.3
Cycle 2	34.6	27.3	10.8	0.9	3.3	9.0	11.9	2.2

Table S2. Textural properties of the catalyst used for the recycling study. R2: after two cycles with calcination step between cycles. "non calcined": with no calcination step between each cycle.

Catalyst	S_{BET} (m^2 g^{-1})	S_{micro} (m^2 g^{-1})	V_{micro} (cm^3 g^{-1})	V_{meso} (cm^3 g^{-1})
Sn-β	632	422	0.172	0.892
Sn-β R2	596	356	0.156	1.197
Sn-β_non calcined	516	316	0.132	0.951

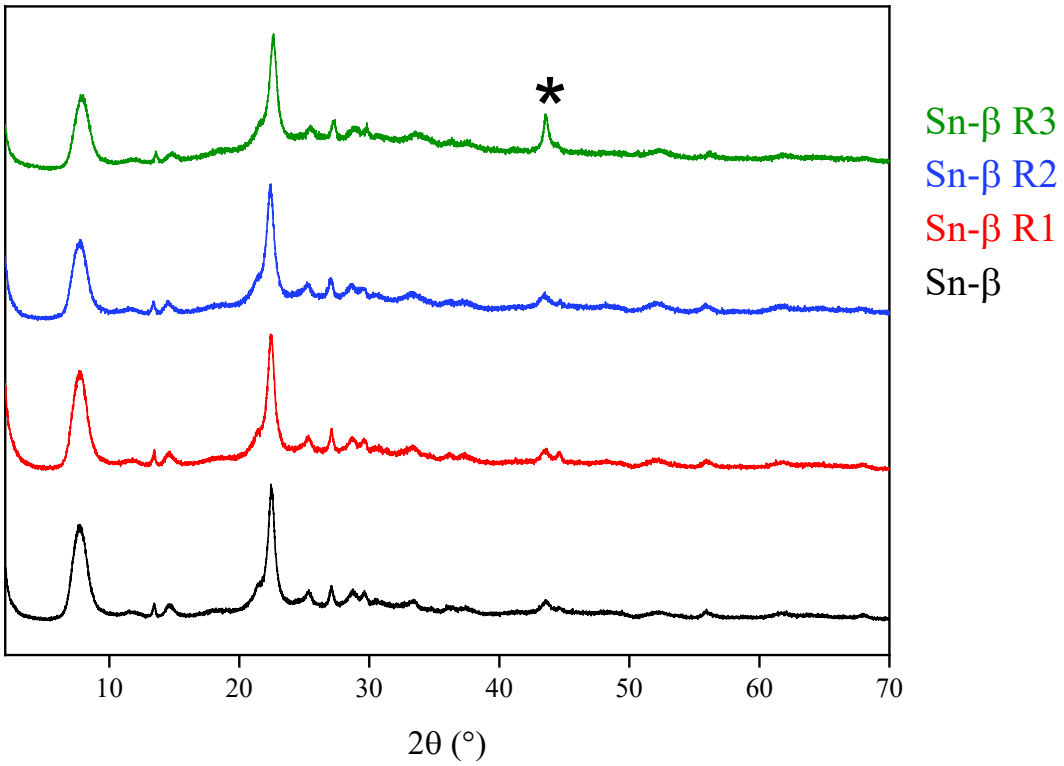

Figure S9. Diffractograms of Sn-β-SSI_1.0 after recycling with calcination step between catalytic test i in R_i indicates the recycling number of the catalyst. * 2θ = 43.6° is a signature of the sample holder.

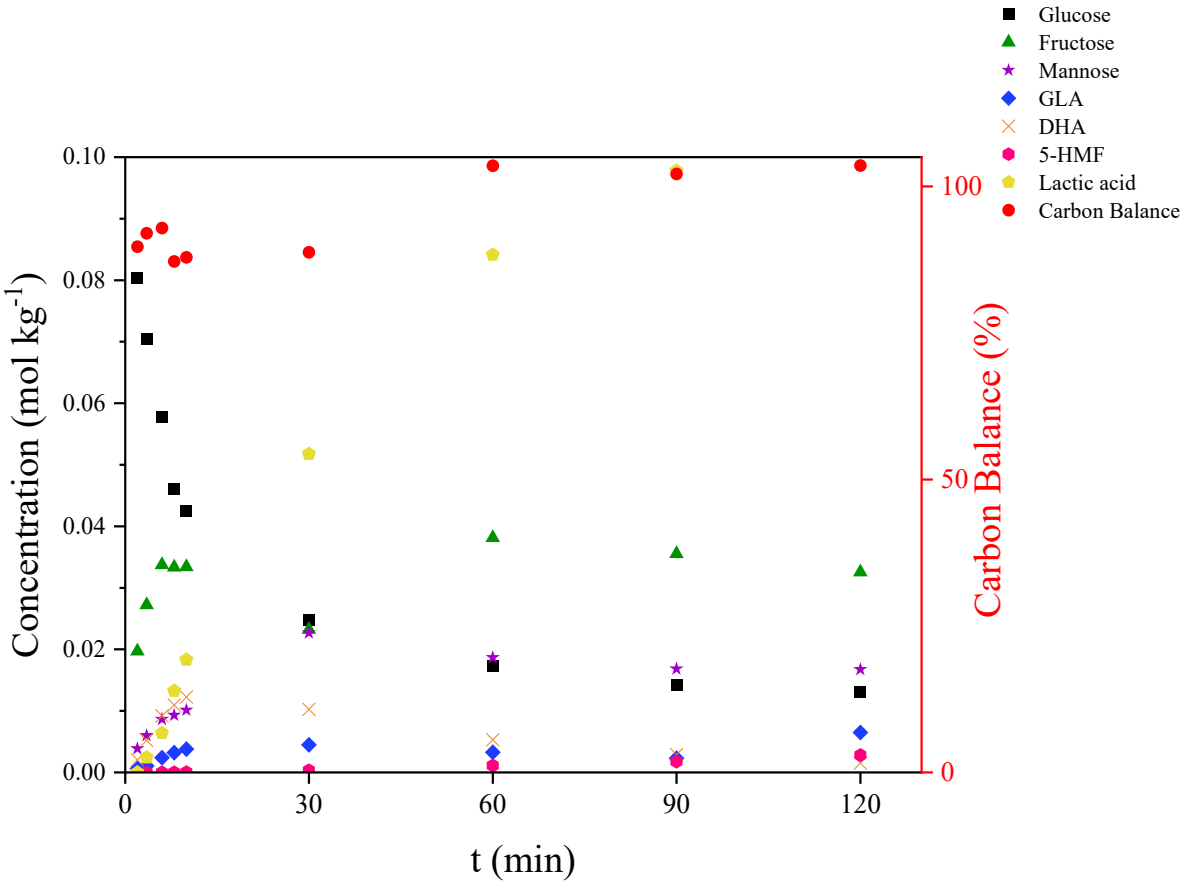

Figure S10. Glucose conversion versus time over **Sn-β-SSI_0.3** in water. Reaction conditions: T= 150 °C, P= 40 bar N_2, concentration of glucose 0.1 mol kg^{-1} and substrate/metal = 100 mol/mol (m_{cat} =2.6311 g) .

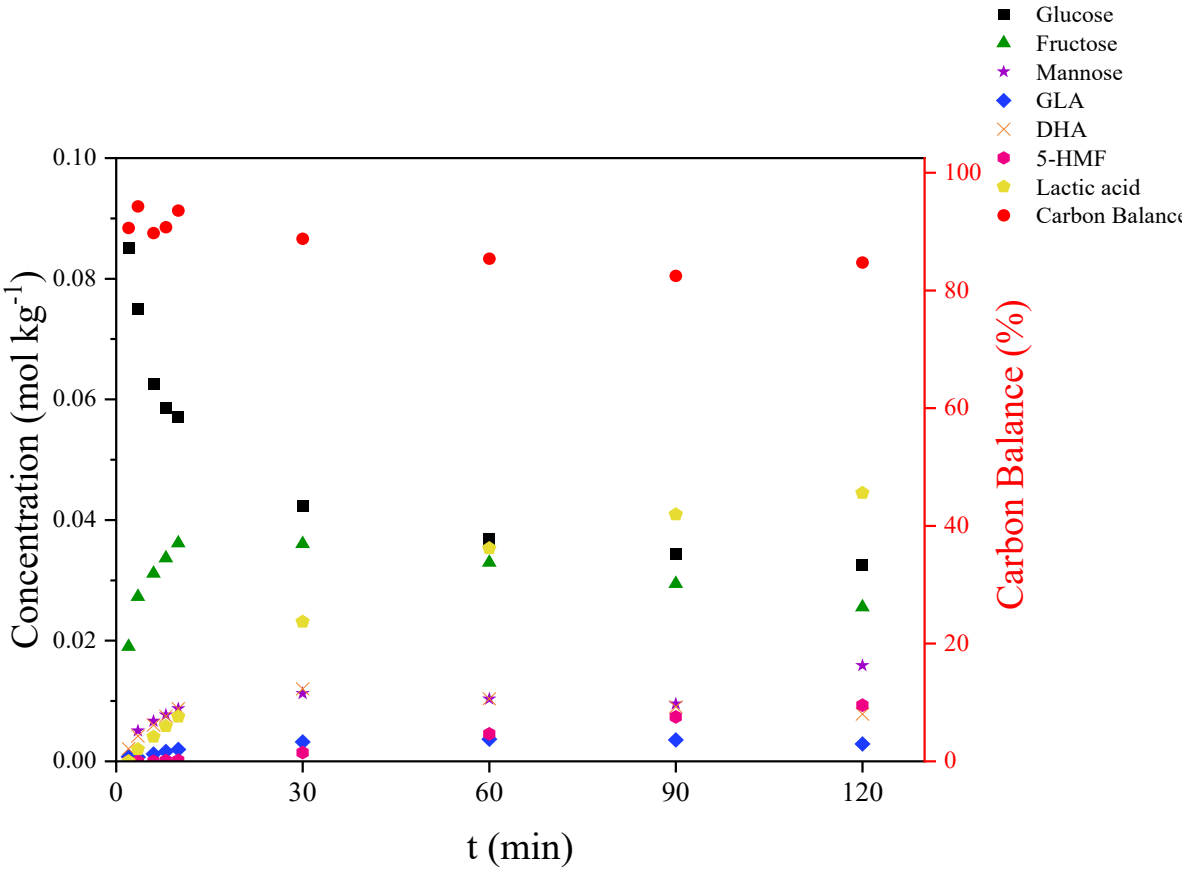

Figure S11. Glucose conversion versus time over **Sn-β-SSI_1.5** in water. Reaction conditions: T= 150 °C, P= 40 bar N_2, concentration of glucose 0.1 mol kg^{-1} and substrate/metal = 100 mol/mol (m_{cat} =0.5271 g).

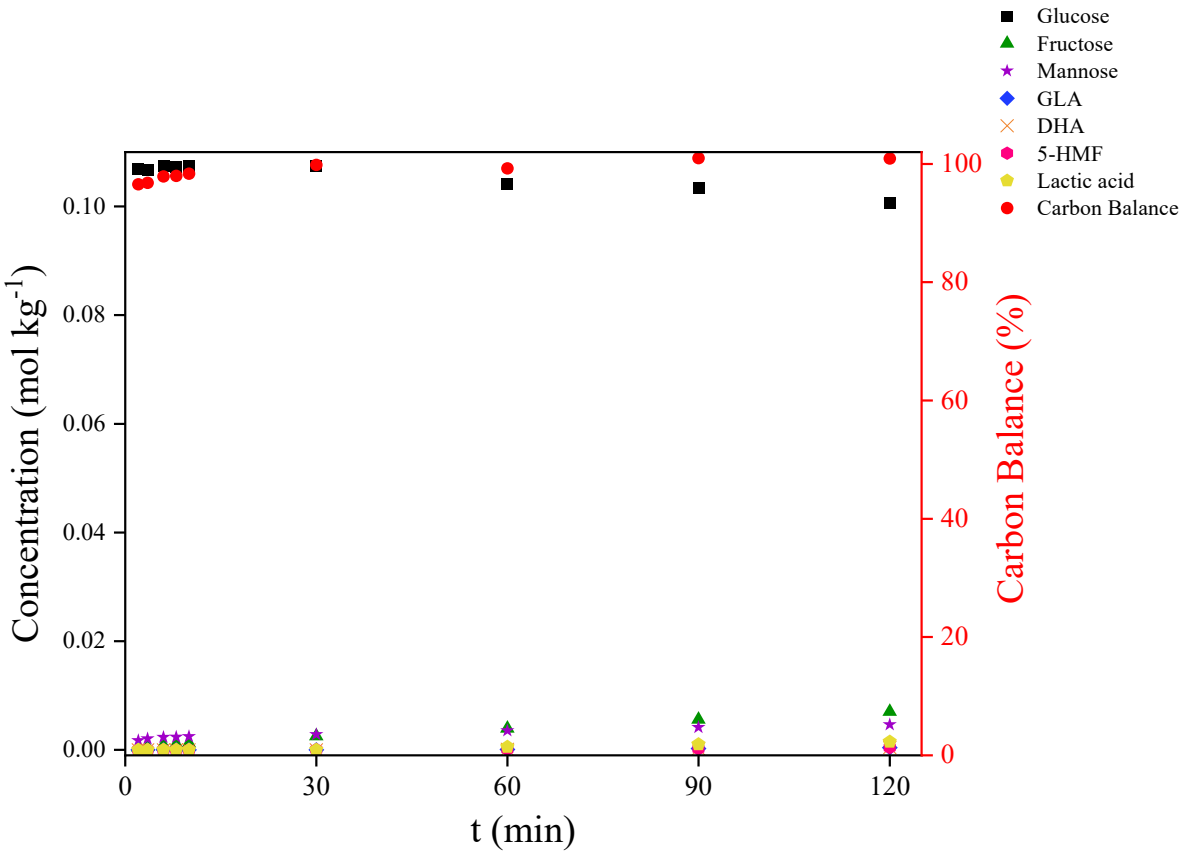

Figure S12. Glucose conversion versus time over **Sn-β-SSI_SnO_2** in water. Reaction conditions: T= 150 °C, P= 40 bar N_2, concentration of glucose 0.1 mol kg^{-1} and substrate/metal = 100 mol/mol (m = 0.7907 g).

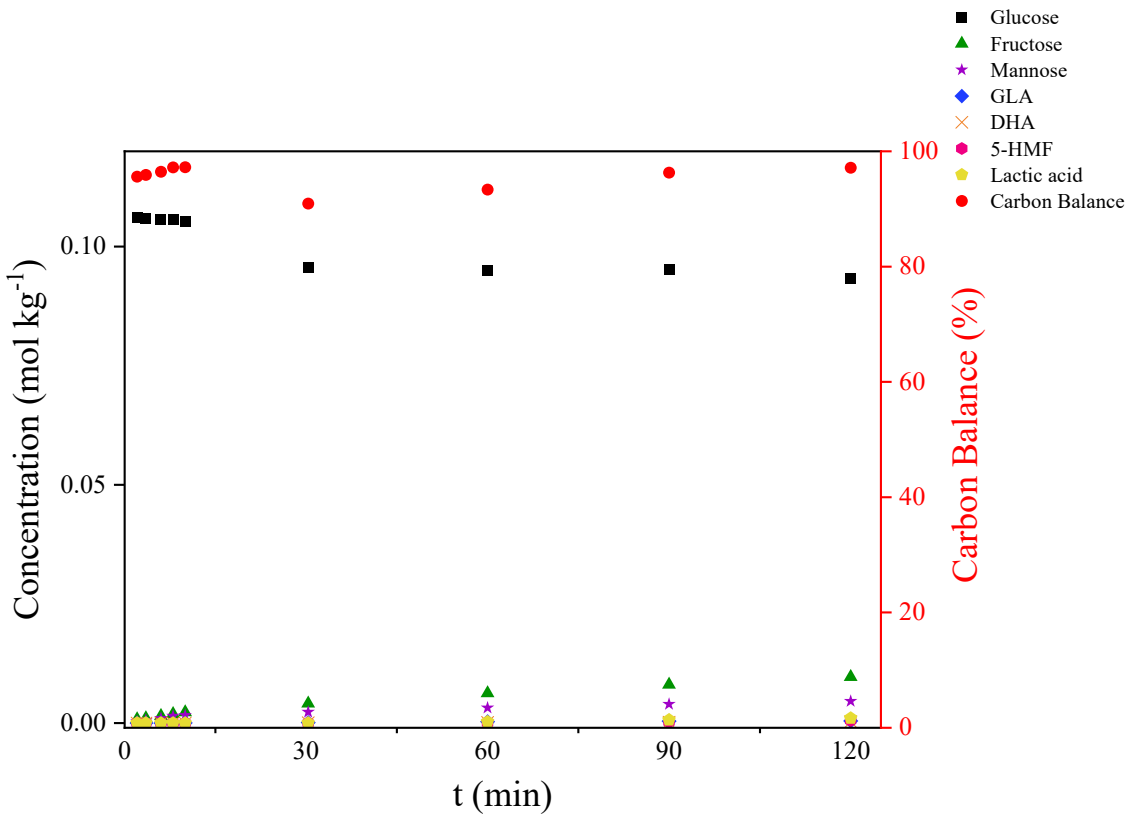

Figure S13. Glucose conversion versus time over **Sn-β-SSI_Sn(OEt)$_2$** in water. Reaction conditions: T= 150 °C, P= 40 bar N_2, concentration of glucose 0.1 mol kg^{-1} and substrate/metal = 100 mol/mol (m = 0.7904 g).

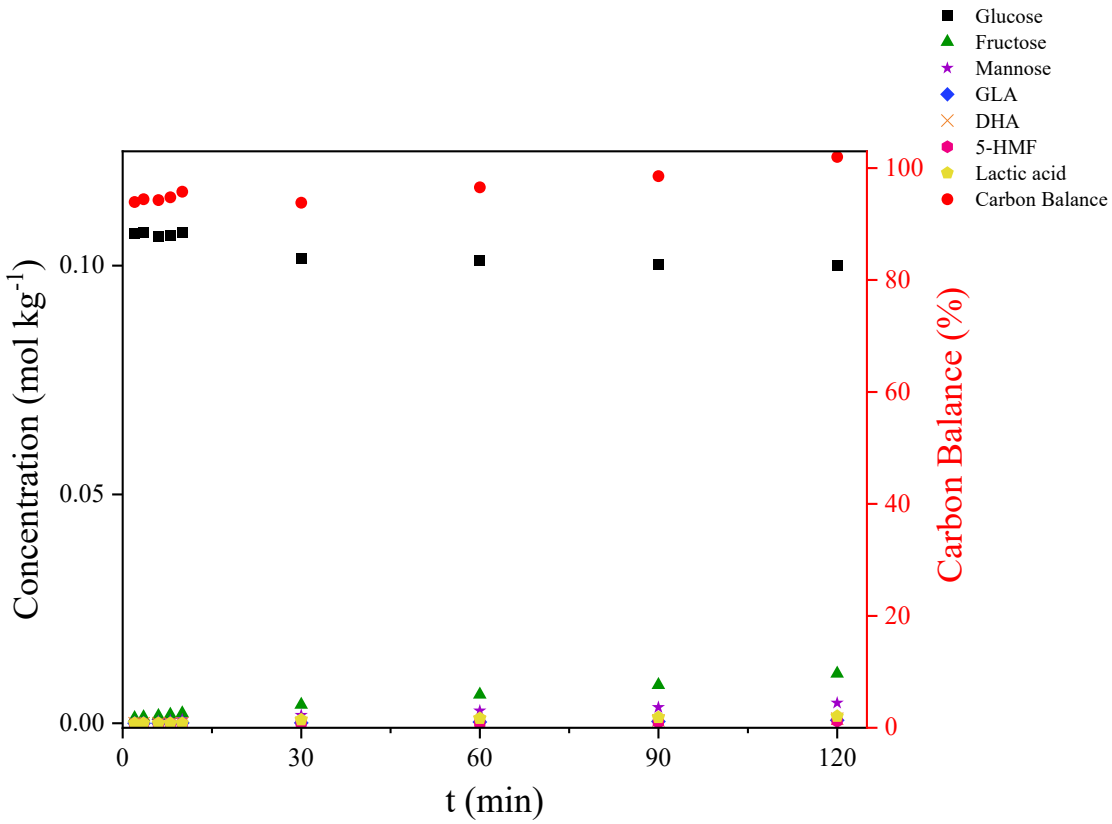

Figure S14. Glucose conversion versus time over **Sn-β-EAI_Sn(OEt)$_2$** in water. Reaction conditions: T= 150 °C, P= 40 bar N_2, concentration of glucose 0.1 mol kg^{-1} and substrate/metal = 100 mol/mol (m_{cat} =0.6932 g).

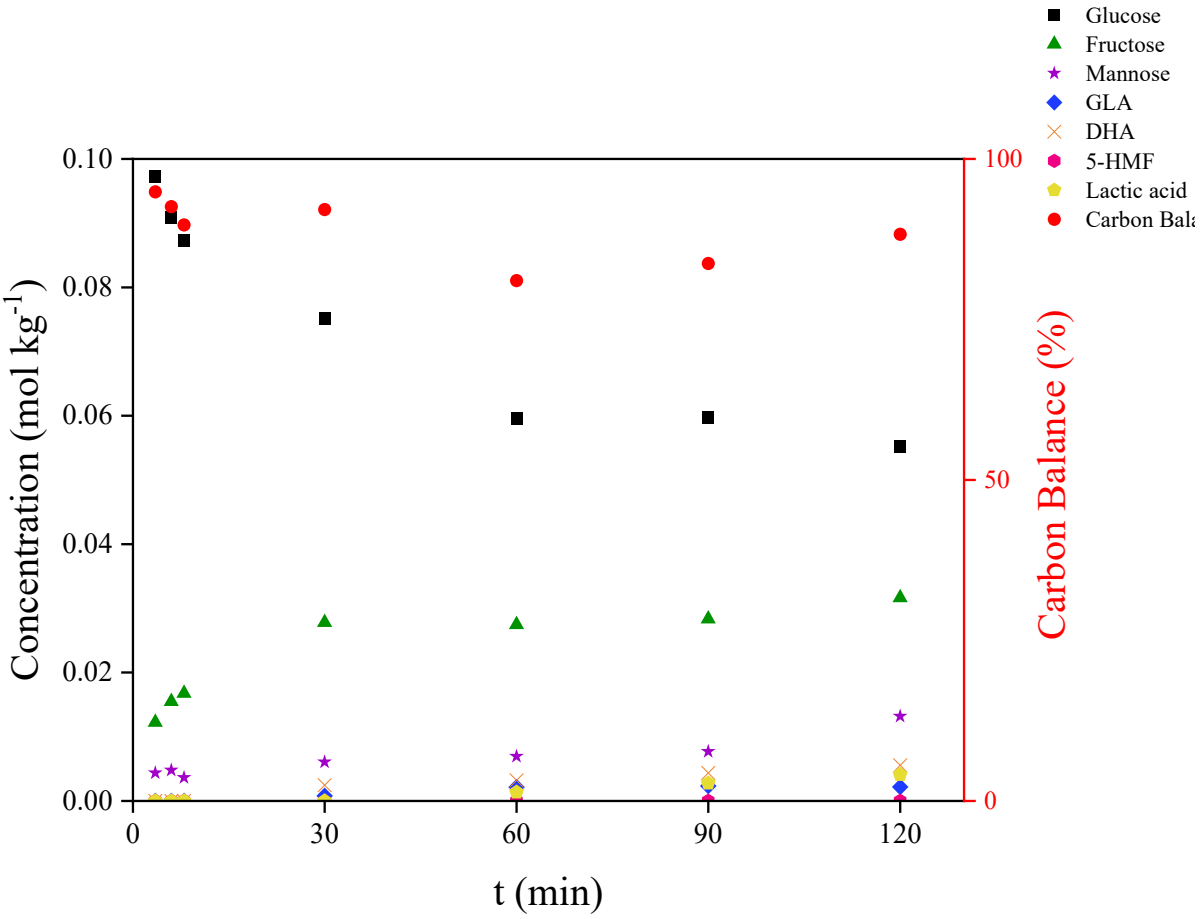

Figure S15. Glucose conversion versus time over **Sn-β-HT** in water. Reaction conditions: T= 150 °C, P= 40 bar N_2, concentration of glucose 0.1 mol kg^{-1} and substrate/metal = 100 mol/mol (m_{cat} =0.7758 g).

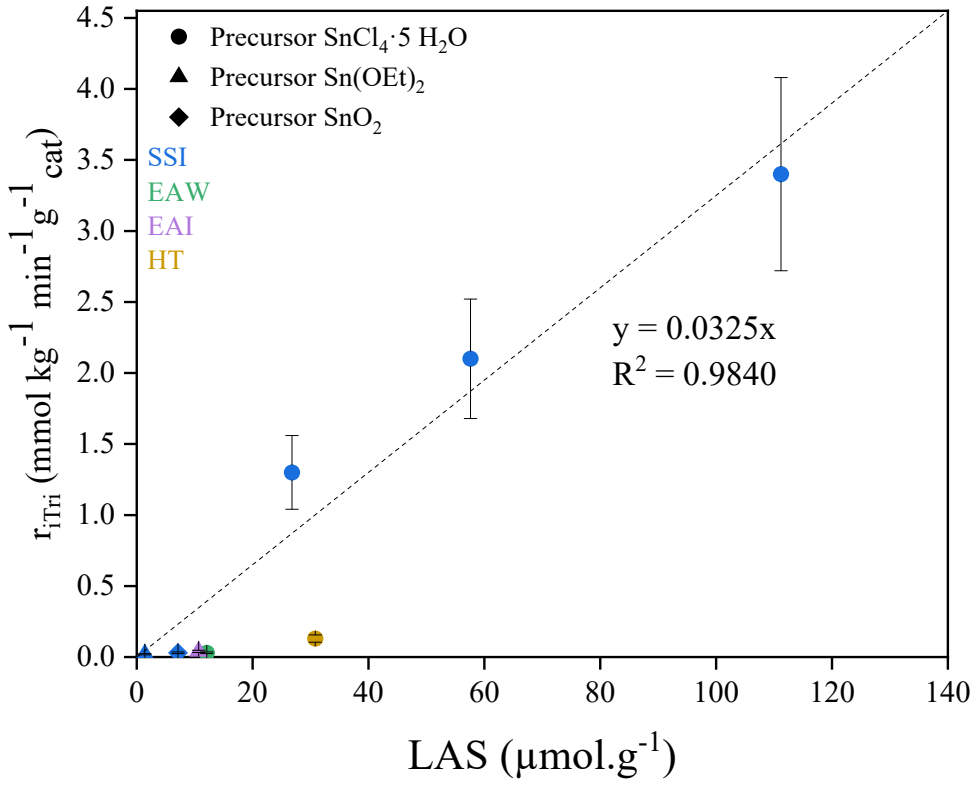

Figure S16. Initial rate of C3 molecules (DHA+GLA+LA) production at 150 °C as a function of the concentration of Lewis acid sites with Sn-β SSI (blue), Sn-β EAW (green), Sn-β EAI (purple), Sn-β HT (yellow), square: precursor $SnCl_4 \cdot 5\ H_2O$, triangle : precursor $Sn(OEt)_2$ and diamond : precursor SnO_2 **;** r_{iTri}: Initial rate of production of trioses ; dashed line : linear fit between Sn-β-SSI_$Sn(OEt)_2$, Sn-β-SSI_1, Sn- β-SSI_1.5 and Sn-β-SSI_0.3.

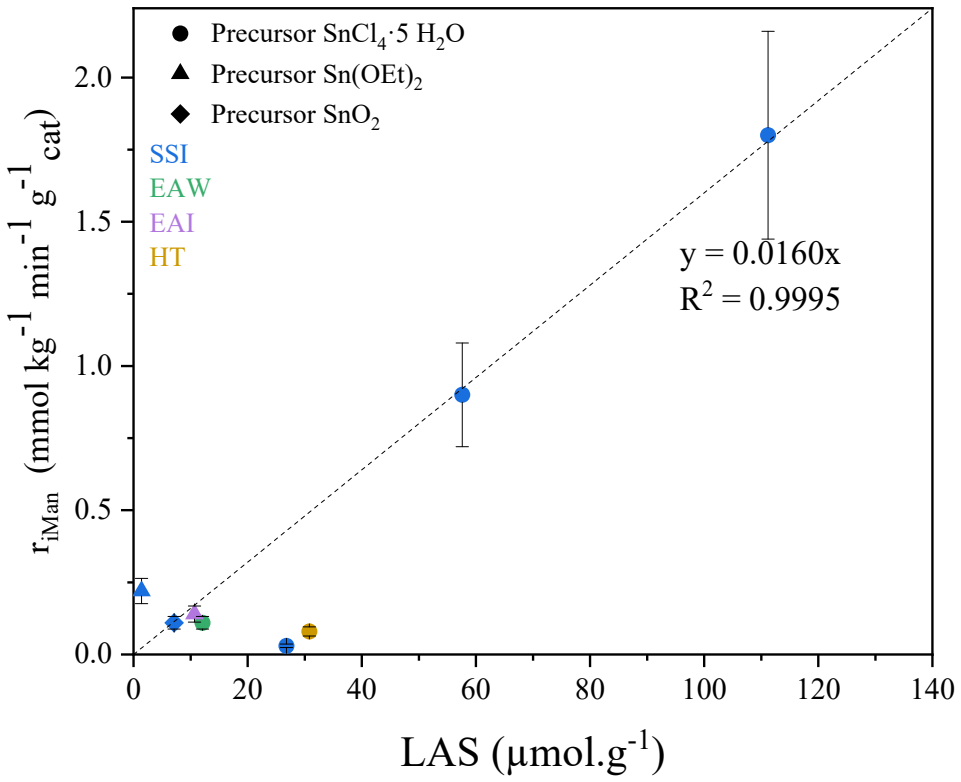

Figure S17. Initial rate of mannose production at 150 °C as a function of the concentration of Lewis acid sites with Sn- β SSI (blue), Sn-β EAW (green), Sn-β EAI (purple), Sn-β HT (yellow), square : precursor $SnCl_4 \cdot 5\ H_2O$, triangle : precursor $Sn(OEt)_2$ and diamond : precursor SnO_2; r_{iMan} : Initial rate of production of mannose; dashed line : linear fit between Sn-β-EAI_$Sn(OEt)_2$, Sn-β-SSI_1, Sn-β-SSI_1.5 and Sn-β-SSI_SnO_2.

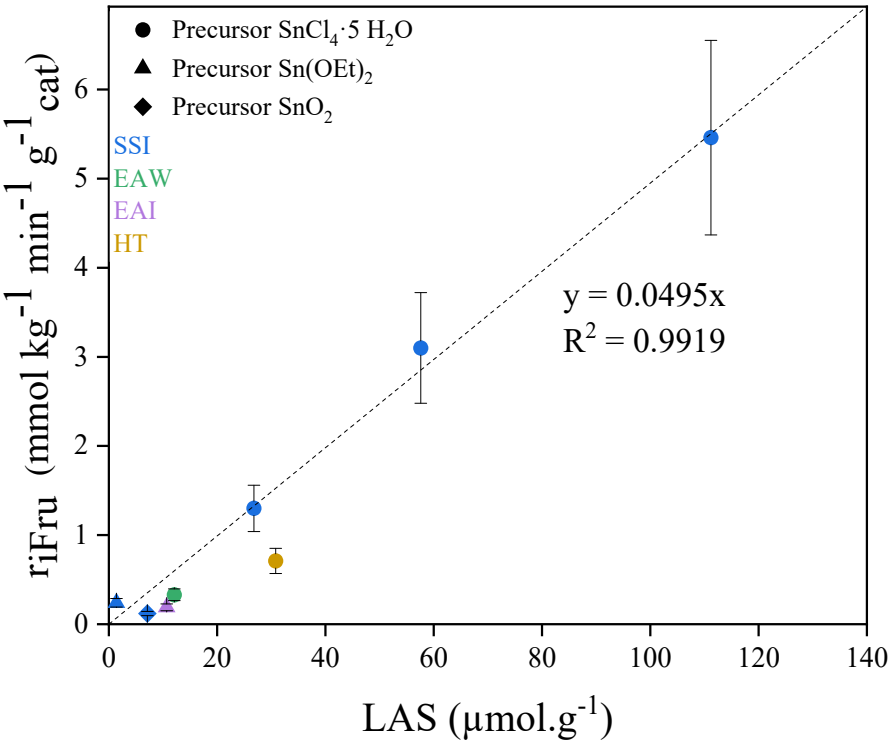

Figure S18. Initial rate of fructose production at 150 °C as a function of the concentration of Lewis acid sites with Sn-β-SSI (blue), Sn-β-EAW (green), Sn-β-EAI (purple), Sn-β-HT (yellow), square : precursor $SnCl_4 \cdot 5\ H_2O$, triangle : precursor $Sn(OEt)_2$ and diamond : precursor SnO_2 ; r_{iFru} : Initial rate of production of fructose ; dashed line : linear fit between Sn-β-SSI_$Sn(OEt)_2$, Sn-β-EAI_$Sn(OEt)_2$, Sn-β-SSI_SnO_2, Sn-β-SSI_1.0, Sn-β-SSI_1.5, Sn-β-SSI_0.3 and Sn-β-EAW.

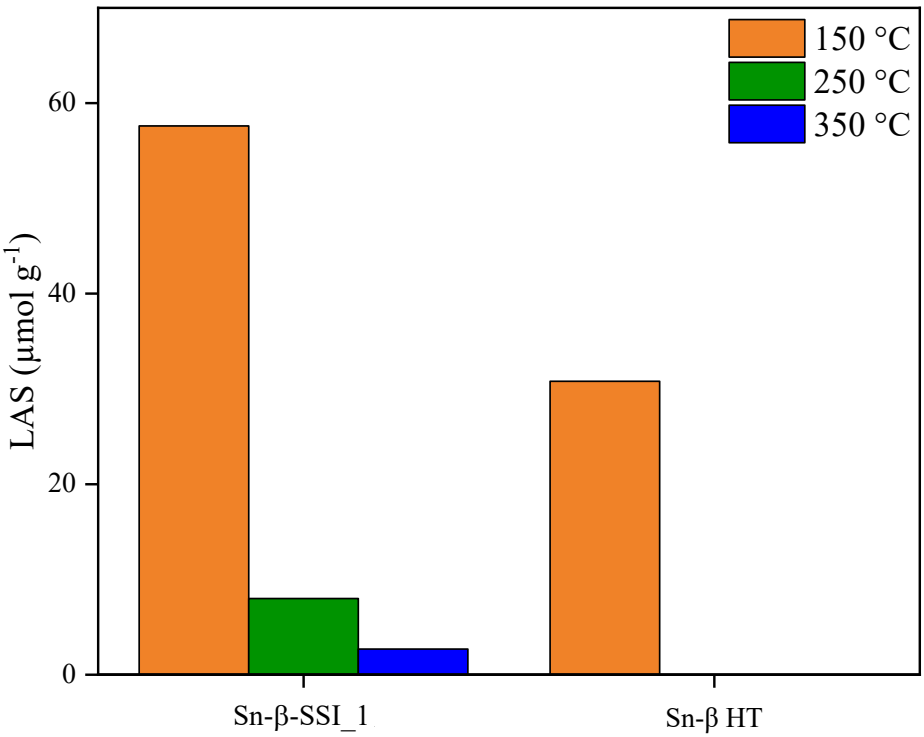

Figure S19. LAS of Sn-β-SSI_1.0 and Sn-β-HT , probed by FTIR spectroscopy of pyridine adsorption and evacuation at 3 different temperatures.

References

1. V. G. Pangarkar, A. A. Yawalkar, M. M. Sharma and A. A. C. M. Beenackers, *Industrial Engineering Chemistry Research*, 2002, **41**, 4141.
2. M. E. Davis, *Fundamentals of Chemical Reaction Engineering,*, McGraw-Hill Higher Education, Boston, 2003.
3. R. Netrabukkana, K. Lourvanij, G. L. Rorrer, *Industrial Engineering Chemistry Research*, 1996, **35**, 458.